IOPscience iopscience.iop.org

Home Search Collections Journals About Contact us My IOPscience

Superparamagnetic nanoparticles and clusters of a few Fe atoms in amorphous $Fe_{0.33}Zr_{0.67}$ alloys

This article has been downloaded from IOPscience. Please scroll down to see the full text article.

1995 J. Phys.: Condens. Matter 7 3315

(http://iopscience.iop.org/0953-8984/7/17/014)

View the table of contents for this issue, or go to the journal homepage for more

Download details:
IP Address: 171.66.16.179
The article was downloaded on 13/05/2010 at 13:01

Please note that terms and conditions apply.

J. Phys.: Condens. Matter 7 (1995) 3315–3326. Printed in the UK

Superparamagnetic nanoparticles and clusters of a few Fe atoms in amorphous $Fe_{0.33}Zr_{0.67}$ alloys

K Rhie†‖, D G Naugle†, B-H O‡¶, J T Markert‡, A H Morrish§ and X Z Zhou§

† Department of Physics, Texas A&M University, College Station, TX 77843-4242, USA
‡ Department of Physics, University of Texas at Austin, Austin, TX 78712, USA
§ Department of Physics, University of Manitoba, Manitoba, Canada

Received 13 September 1994

Abstract. A paramagnetic amorphous $Fe_{0.33}Zr_{0.76}$ alloy has been studied with Mössbauer spectroscopy and SQUID magnetometry. Low-field magnetization measurements revealed the existence of superparamagnetic nanoparticles of thousands of μ_B embedded in the alloy with a blocking temperature of 50 K. A saturation of local moments ($15.9\mu_B$), possibly clusters of a few Fe ions, is observed at 4.6 K around 10 kOe. The temperature dependence of the high-field magnetic susceptibility of $Fe_{0.33}Zr_{0.67}$ is interpreted with Curie's law for these Fe clusters and nanoparticles.

1. Introduction

The Fe–Zr amorphous metallic alloys have attracted attention in spin glass studies and Mössbauer spectroscopy because of the wide concentration range for forming the amorphous phase and the variety of magnetic behaviour that can be achieved by changing Fe content [1–3]. This alloy system experiences paramagnetic, spin glass and ferromagnetic phases as the Fe content increases. The spin glass transition from the paramagnetic state to a ferromagnetic state occurs at much higher Fe content, 42.8 at.% [3]. Recent Mössbauer spectroscopy [1, 4] and anomalous scattering studies [5] indicate that the magnetic environment of Fe ions starts to change at an Fe concentration of 33 at.% and that the direct Fe–Fe interaction starts to appear at the same concentration.

A Curie–Weiss-like temperature-dependent paramagnetic susceptibility with a negative Curie temperature Θ [6, 7] in a high magnetic field is reported near this Fe concentration. Such negative Curie temperatures are reported frequently near the ferromagnetic boundary composition; $Ni_{0.80}P_{0.20}$ [8], $Ni_{0.80}P_{0.14}B_{0.06}$ [9] and $Co_{0.60}Zr_{0.40}$ [10] alloys provide other examples of this behaviour. This negative Θ is questionable and totally non-physical in the Weiss mean-field approach unless antiferromagnetic order is present, which is not the case for the amorphous transition-metal-based alloys. Several reasons for this temperature dependence can be proposed: a temperature-dependent Stoner enhancement, superparamagnetic particles, clusters and local Kondo impurities. The $Fe_{0.33}Zr_{0.67}$ alloy studied here is paramagnetic and its susceptibility shows a large temperature dependence. The temperature and field dependence of the magnetization of this alloy is reported and

‖ Present address: Department of Physics, Korea University, Jochiwon, Choong-Nam, 339-700 Korea.
¶ Present address: Department of Electronic Materials, Inha University, Inchon, Korea.

0953-8984/95/173315+12$19.50 © 1995 IOP Publishing Ltd

analysed in terms of superparamagnetic particles and clusters embedded within the alloy. In this article we adopt the definition for a particle or nanoparticle as a group of atoms that exhibit a magnetic coherence over a region greater than 6.5 nm whereas a cluster refers to a smaller group of coupled magnetic moments extending to a single isolated magnetic impurity. This is consistent with the terminology given in the literature [11].

One possible source of Curie–Weiss-like temperature dependence is clusters of Fe ions, which make direct contact and do not have the short-range order associated with the Zr_2Fe structure. These directly connected Fe ions can exhibit local moments once a Fe ion is kicked out from the Zr neighbours that used to surround it. In this case, small clusters of Fe ions bonded magnetically by the direct exchange interaction will follow the Curie law, if the interaction between the neighbouring Fe clusters is sufficiently weak that the clusters can be treated as independent of each other. These small clusters can be saturated only at low temperature and high fields. Otherwise, they are bonded by direct exchange interaction and will form few Fe groups. The present measurements suggest that clusters of very few Fe ions dominate the high-field susceptibility for these alloys over the whole temperature region.

2. Experiment

The $Fe_{0.33}Zr_{0.67}$ ingots were prepared by arc melting appropriate amounts of 99.996% pure Fe and 99.6% pure Zr in an Ar atompsphere. The ribbons were melt spun in a single-roller melt spinner at a wheel speed of about 30 m s^{-1}. A typical sample width was 3 mm with a thicknesss of 18–23 μm. The samples were cut into 0.6–0.8 cm lengths by the fold cutting method, in order to rule out the possibility of introduction of any impurity from the stainless steel scissors. Several short pieces (110 mg) were stacked into a 1 cm long gelatin capsule and mounted in a SQUID magnetometer. The diamagnetic susceptibilty of the capsule was measured separately and subtracted from the raw data. In order to determine whether the results were characteristic of this alloy, the temperature dependence of the magnetization at 10 kOe was measured for three different batches. The results agreed within 1%, i.e. within about the estimated absolute error for these measurements.

The zero-field-cooled and field-cooled measurements were carried out as follows. First, the zero field of the superconducting magnet in the SQUID magnetometer was calibrated with a paramagnetic salt, then the samples was cooled down to 2 K in zero field. A magnetic field of 5 Oe was applied at 2 K. The magnetization was measured as the sample was warmed to 300 K. For the field-cooled measurements the sample was cooled again down to 2 K.

The M–H plot was measured first at 300 K. The magnetic field was changed from 0 Oe to 10 kOe, to −10 kOe and back to zero at each temperature. At 4.6 K, the magnetic field was varied from −50 to 50 kOe in order to look for the effects due to the smallest clusters. The magnetic susceptibility $\chi(T)$ also was measured at 10 kOe by varying the temperature. Usually $\chi(T)$ near the ferromagnetic transition has been fitted to the Curie–Weiss law, even though the physical meaning of the negative Θ is not clear.

^{57}Fe Mössbauer spectra were collected from room temperature down to 1.8 K (pumped liquid He) and also at 4.2 K in an applied magnetic field of 50 kOe. The spectrometer was operated in the constant-acceleration mode using a sinusoidal drive and calibrated with an α-Fe foil at room temperature. The source was ^{57}Co in an Rh host. Each spectrum was folded and analysed with a least-squares computer program.

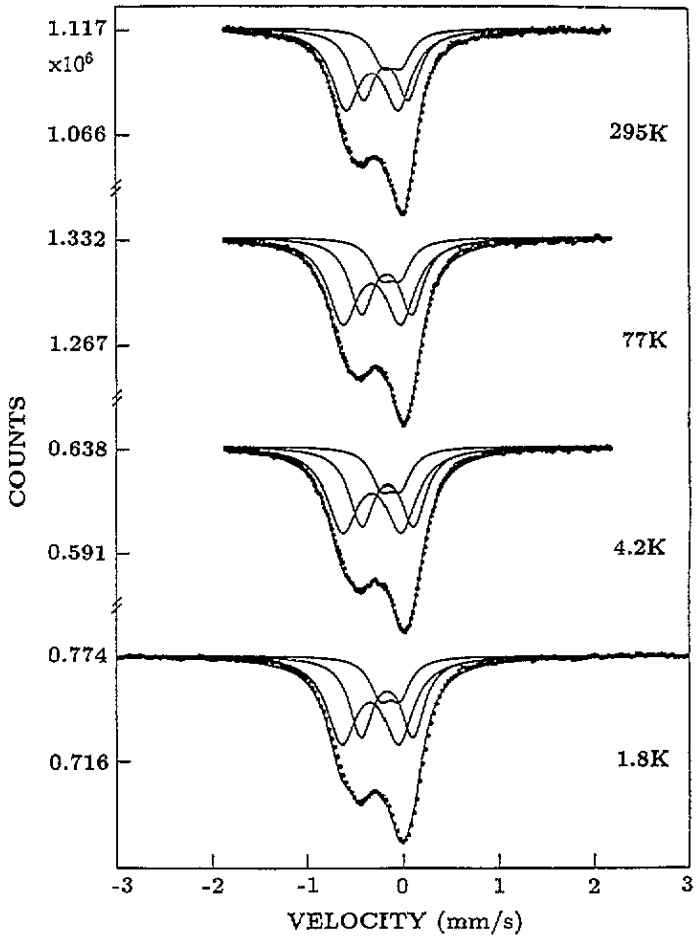

Figure 1. Mössbauer spectra of $Fe_{0.33}Zr_{0.67}$ at various temperatures as indicated in the figure. The points represents the experimental data and the full curves the three doublets and their sum as obtained in a least-squares computer fit.

3. Results and discussion

3.1. Superparamagnetic nanoparticles

The Mössbauer spectra of the $Fe_{0.33}Zr_{0.67}$ alloy at temperatures of 295, 77, 4.2, and 1.8 K are shown in figure 1. No magnetic hyperfine split patterns are detectable; instead only a central absorption is observed. Therefore, according to this technique, the alloy is in a paramagnetic state even down to 1.8 K. The Arrot plot for the $Fe_{0.33}Zr_{0.67}$ alloy at 4.6 K, as obtained from the SQUID measurements, is shown in figure 2. This Arrott plot also indicates that paramagnetism is dominant for $Fe_{0.33}Zr_{0.67}$.

A superparamagnetic particle is one that has ferrimagnetic or ferromagnetic order but has a moment that fluctuates (rapidly) from thermal agitation. However, below the blocking temperature it behaves as a single domain that will respond to an applied magnetic field. This applied field will rotate the magnetization of the particle towards alignment with the field where the details are determined by the anisotropy and orientation. In the analysis

of magnetism in $Fe_{0.33}Zr_{0.67}$ we will assume that superparamagnetic particles, most likely nanoparticles and very small clusters, are embedded in a non-magnetic amorphous matrix. The nanoparticles need not be crystalline arrangements of atoms, but their size and quantity are expected to be below the detectability level associated with most techniques for structural analysis. Below the blocking temperature, the magnetization of the alloys should show non-linearity at low field, if superparamagnetic particles are present. At high magnetic field, these moments will be saturated. To see whether the magnetic properties of $Fe_{0.33}Zr_{0.67}$ could be described in terms of a collection of superparamagnetic particles embedded in the amorphous matrix, M–H data were fitted using the equation

$$M = \chi_{HF}(T)H + \sigma(H, T)$$

where

$$\sigma = \sum_i \sigma_i = \sum_i N_i \mu_i \left\{ \coth\left(\frac{\mu_i H}{k_B T}\right) - \frac{k_B T}{\mu_i H} \right\} = N^* \mu^* \left\{ \coth\left(\frac{\mu^* H}{k_B T}\right) - \frac{k_B T}{\mu^* H} \right\} \qquad (3.1)$$

where i stands for different kinds of particle or nanoparticle. $\chi_{HF}(T)$ stands for the temperature-dependent linear magnetic susceptibility at high fields and the non-linear part σ represents the magnetization of the particles. The magnetic moments of the sample above the blocking temperature should be described by the Langevin function if magnetic moments of the particles are identical. Clearly a statistical distribution of size and magnetic moment of the particles is expected. We define the effective moment μ^* and number density N^* of the clusters at a given temperature as that given from a fit to (3.1) of the magnetization as a function of field at fixed temperature. Since different-size particles will tend to dominate the field dependence at different temperatures, the effective moment and density, although artificial, are still useful concepts. The magnetic susceptibility at high field ($\chi_{HF}(T)$) is the sum of the Pauli paramagnetic contribution from the conduction band and a Curie paramagnetic term from relaxed clusters of a small number of Fe ions with $\mu H/k_B T \ll 1$, as well as the Van Vleck and diamagnetic contributions.

Table 1. H/T when the magnetic energy is comparable to the thermal energy or 90% of moments are saturated for different kinds of moment. Note that the argument of the Brillouin function varies with the J value when $B_J(\mu H/k_B T) = 0.9$. Note that larger moments saturate at smaller magnetic field, so the large particles saturate at a magnetic field lower than 100 Oe at liquid He temperature.

Kinds of local moment	Typical moment size (μ_B)	When $\mu H/k_B T = 1$ H/T (Oe K^{-1})	When $B_J(\mu H/k_B T) = 0.9$	
			$\mu H/k_B T$	H/T (Oe K^{-1})
Electron ($J = \frac{1}{2}$)	1	1.5×10^4	1.46	2.1×10^4
Fe ion ($J = 2$)	4	3.7×10^3	3.56	1.3×10^4
Cluster of $J = 5 \times 10^3$	10^4	1.5	10.0	1.5×10

It is convenient to make a table of the H/T ratio for different sizes of magnetic moments when the magnetic energy is equal to the thermal energy, so that one can deduce which size moment is dominant for given H and T. The effective magnetic moment deduced from (3.1) is of the order of $10^4 \mu_B$ while that for a single Fe ion would be about $4\mu_B$ assuming that $J = 2$ and the Landé g factor is two. Table 1 shows these values for a single electron, an Fe ion and a nanoparticle with $J = 5000$. For example, a single Fe ion at 4 K requires

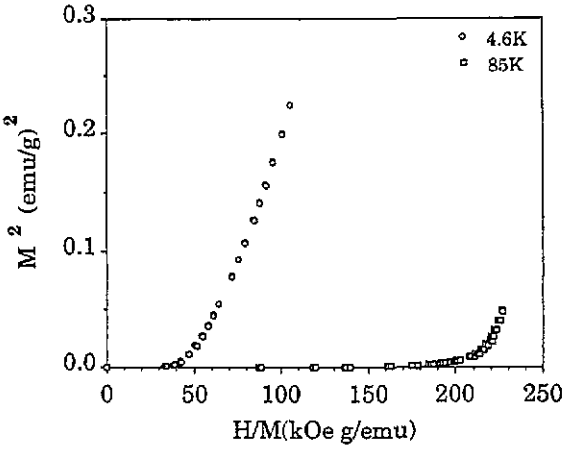

Figure 2. Arrot plots at 4.6 K and 85 K, showing that $Fe_{0.33}Zr_{0.67}$ is paramagnetic.

at least 14 kOe to overcome the thermal energy and start to align, and at 300 K, 5 kOe is enough to align 90% of the nanoparticles with $J = 5000$.

The room-temperature magnetization in figure 3(a) seems linear throughout the whole magnetic field range (−10–10 kOe), but the low-temperature values (figure 3(b)) clearly show saturation of a small impurity moment in the range of −1–1 kOe. The Langevin function does not fit very well to the low-field data for $T \leqslant 50$ K. Furthermore, a small hysteresis was measured at 10 K (the inset in figure 3(b)). According to Néel [12] the coercive field for a system of spherical particles with cubic anisotropy and oriented randomly is $H_c = 0.64K/M_s$ where K is the anisotropy constant and M_s is the saturation magnetization. These nanoparticles, presumably in the range of 6.5 nm if α-Fe, would have an H_c of about 170 Oe [11], which is consistent with the experimental result. This is strong evidence for the existence of the superparamagnetic clusters made of α-Fe. The limit of the sensitivity of the Mössbauer experiment is at best 1% of the signal. In figure 1 the third doublet comprises about 15% of the total area, and yet a reasonable fit to the data can be obtained without it. Consequently, the Mössbauer data are completely insensitive to the Fe in the superparamagnetic nanoparticles, which we estimate comprise less than 0.1% of the total Fe atoms in the sample.

The net saturation moment of the nanoparticles $\sigma(T)$ and the effective moment of a single nanoparticle μ^* from the fitting to (3.1) are shown in figures 4 and 5, respectively. $\sigma(T)$ increases as the temperature decreases, as expected, since particles of smaller moment will saturate at lower temperatures. However, the effective moment of the nanoparticles μ^* increases up to 50 K and then starts to decrease with T.

In connection with the maximum in μ^* at 50 K, the splitting of the zero-field-cooled and field-cooled data occurs at 45 K (figure 6). The AC susceptibility measurements of [3] indicate that the spin glass transition occurs below 20 K for $Fe_{0.428}Zr_{0.572}$. It is hard to believe that a spin glass transition occurs at 50 K in the $Fe_{0.33}Zr_{0.572}$ alloy. We suppose that this split is due to the blocking of larger moments.

3.2. Local Fe moments

It is interesting to see that the net saturation moment $\sigma(T)$ in figure 4 becomes larger for lower temperature, while the effective moment of a single cluster decreases with decreasing

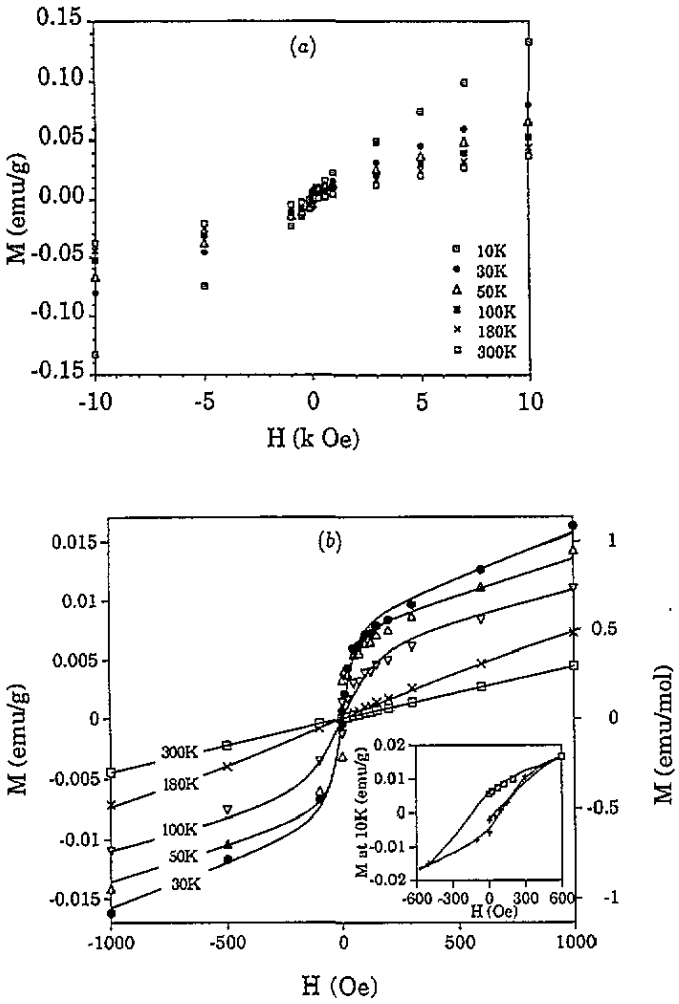

Figure 3. (*a*) M against H at several temperatures. (*b*) Blown up from (*a*) for small applied field. The line is the Langevin function fit to (3.1). The inset shows hysteretic behaviour at 10 K. The value of the coercive force is almost the same as the value expected for single-domain particles of α-Fe.

temperature at $T \leqslant 50$ K. This result reflects the fact that the number of smaller local moments is quite large, and that they dominate at the lower temperature. The M–H plot at 4.6 K in figure 7 provides confirmation. AT 4.6 K the magnetization starts to saturate around 10 kOe. The particles with large moments are already saturated at higher temperatures, but their contribution to the total magnetization is negligibly small compared to that of this smaller moment, which saturates at lower temperatures. (Note that the saturation moment in figure 7 is an order of magnitude greater than those given in figure 4.) The magnetization curve in figure 7 was fitted to a Brillouin function, taking the J value and cluster density n as variables along with the background paramagnetic slope due to the Pauli, diamagnetic and Van Vleck contributions to the susceptibility, i.e.

$$M = (\chi_{\text{Pauli}} + \chi_{\text{dia}} + \chi_{\text{Van Vleck}})H + ngJ\mu_B B_J(gJ\mu_B H/k_B T). \qquad (3.2)$$

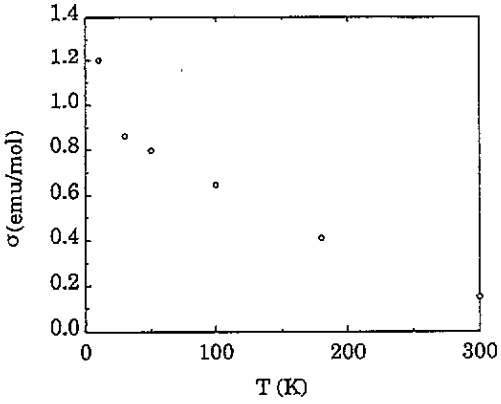

Figure 4. Saturated moment against temperature from $M-H$ plots at several temperatures.

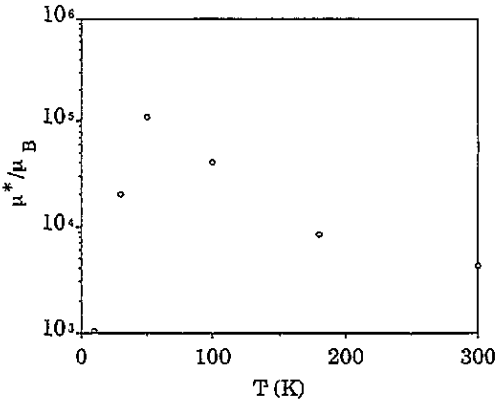

Figure 5. The effective moment of the nanoparticles embedded in the alloy in Bohr magneton units (μ_B) at several temperatures.

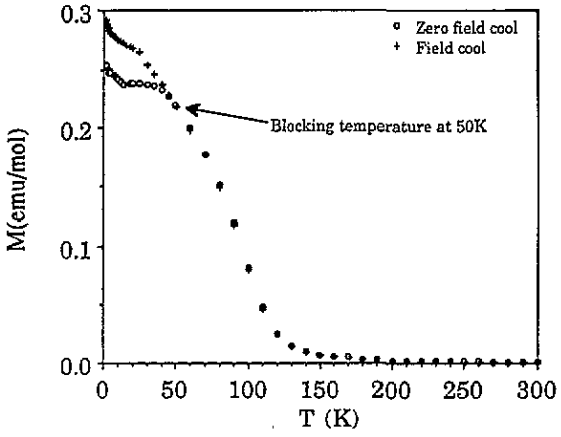

Figure 6. Zero-field-cooled and field-cooled data split at 45 K, near the temperature for the maximum of the effective moment of the nanoparticles as shown in figure 5.

The best fit was obtained with $gJ\mu_B = 15.9\mu_B$, $n = 190$ ppm and a high-field slope $\chi_{Pauli} + \chi_{dia} + \chi_{Van\ Vleck} = 466$ μemu mol^{-1}. The g value is three or four times larger than that of a single Fe ion with $S = 2.5$ or 2. The high-field paramagnetic slope is smaller than the value at 10 K (figure 8), since the last term of (3.2) becomes linear with H and merges with the linear high-field susceptibility as T increases. These two terms are inseparable from one another numerically at high enough temperature. The total saturation due to the last term of (3.2) is 15.67 emu mol^{-1} at 4.6 K. This is about 20 times larger than the net saturation of clusters at 50 K, where μ^* was a maximum. The contribution of those nanoparticles with large μ^* to (3.2) is neglected, because the net saturation value is small compared to the saturation moment from the small clusters with $\mu = 15.9\mu_B$ at this temperature. The excellent fit in figure 7 suggests an abundance of local moments of the order of single Fe ions.

One possible explanation for the observation of effective moments three to four times the

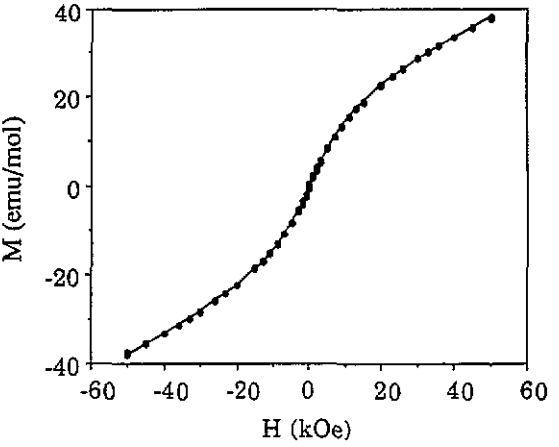

Figure 7. An M–H plot at 4.6 K. Saturation of clusters with very small moments is observed near 10 kOe. The slope in the background is due to the Pauli, diamagnetic and Van Vleck susceptibilities.

size of single Fe moments might be the Stoner enhancement factor. The Stoner enhancement of the Pauli paramagnetic states generates an effective field enhanced by the enhancement factor I, $H_{\text{effective}} = IH_{\text{applied}}$. Consequently, a Stoner enhancement factor of $I \approx 4$ would imply that the effective moment $Ig_0J\mu_B = gJ\mu_B = 15.9\mu_B$ could even be due to moments associated with single ion impurities. This enhancement of applied field does not affect the value of the net saturation of superparamagnetic clusters, but the interpretation of the effective μ^* or coercive factors would be influenced. Weakening of the Stoner enhancement with temperature cannot explain the decrease of μ^* with temperature for $T > 50$ K since the ratio of μ^* at 50 K to that at 300 K is about 20 while the Stoner enhancement factor cannot be larger than four. Neither can the Stoner enhancement explain the decrease of μ^* with T for $T < 50$ K since the temperature dependence of the Stoner-enhanced Pauli state should follow the $1/(T^2 - \Theta^2)$ law.

As alternative explanation for a particle with an effective moment three to four times the size of a single Fe moment would be the existence of a few atoms whose moments are coupled magnetically. If the spins of the three Fe ions are tied together by the exchange interaction, these Fe ions may react to the applied field like a single object.

Since the central absorption in the Mössbauer spectra (figure 1) is asymmetric, at least two double patterns must be present. However, when three doublets are used the goodness of fit parameter, χ^2, decreases by a large amount. For the spectrum at 4.2 K in an applied magnetic field of 50 kOe (not shown), a good fit is also obtained with three patterns using a Hamiltonian with a hyperfine field of 50 kOe and the quadrupole interactions obtained from figure 1, provided the line intensities are integrated for a random powder. These results are in agreement with the earlier measurements by Michaelson *et al* [1] for room-temperature spectra. These authors investigated various compositions of the Fe–Zr systems and observed that the $Fe_{0.33}Zr_{0.67}$ alloy locates the position at which this additional doublet appears; it becomes dominant as the Fe content increases (even in the paramagnetic state). In addition, anomalous scattering studies [5] indicate that at this concentration a direct contact starts to occur between Fe ions. These facts reflect that a new magnetic environment appears as the Fe content approaches 33% and strongly support the idea that the clustering of a few Fe ions can explain moments of this size. Furthermore, we have observed in the previous section

Table 2. The experimental values and the equation used for the total magnetic susceptibility χ_T and high-field magnetic susceptibility χ_{HF}. The Curie constant in the last row is deduced from the effective moment of $15.9\mu_B$ of few-ion clusters.

Experimental values	Equation fitted with	C (10^{-3} emu K mol^{-1})	Θ (K)	α	$\chi_{Pauli+dia+Van\ Vleck} = \chi_0$ (μemu mol^{-1})
$\chi_T = M/H$	$\chi_T = C/(T-\Theta)+\chi_0$	15.0	— 9.83		265
	$\chi_T = C/T^\alpha + \chi_0$	3.2		0.576	183
$\chi_{HF} = \partial M/\partial H$	$\chi_{HF} = C/T + \chi_0$	8.5			263
$C = n\mu_{eff}^2 N_A/3k_BT$ with $\mu = 15.9\mu_B$		5.8			

that the clusters of this smaller moment are more abundant and dominate the magnetic properties at the lower temperatures. One might expect the size of the clusters to extend even to a small group of a few Fe ions. The hard part to explain is then why three or four ions join together, rather than two ions. One possibility is that the separated single Fe ion from the $FeZr_2$ matrix locates in between two Fe ions in the neighbouring amorphous $Fe_{0.33}Zr_{0.67}$ matrix, and connects those two separated Fe ions by an exchange interaction. Stoner enhancement of the effective field for Fe dimers is also a possibility. If these small Fe clusters are the reason for the saturation observed at low temperature (figure 7), the contribution to the Curie constant can be determined from

$$\chi_{Curie} = \mu_{eff}^2 n N_A/3k_BT \text{ (molar susceptibility)} \tag{3.3}$$

where $\mu_{eff} = 15.9\mu_B$. This gives a value of 5.84×10^{-3} emu K mol^{-1} for the Curie constant, which is about two-thirds of the value obtained from the fit to Curie's law of the high-field susceptibility in figure 8 (see table 2). The calculated Curie constant is lower by a factor of three if single Fe moments together with the Stoner enhancement are responsible for the large number of effective moments at the value $\mu = 15.9\mu_B$. The presence of single Fe ions, which would not have saturated at 4.6 K, would help make up the difference between the Curie constant determined from the fit in figure 8 and that calculated for the small clusters with $\mu_{eff} = 15.9\mu_B$.

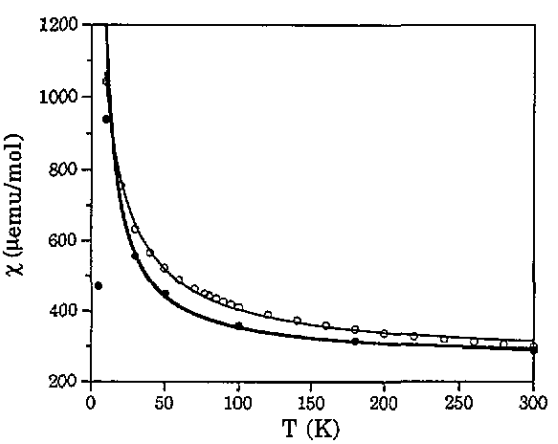

Figure 8. The total magnetic susceptibility ($\chi = M/H$) at 10 kOe (open circles) fitted with the Curie–Weiss expression (thin line). The high-field susceptibility ($\chi = \delta M/\delta H$) near 10 kOe at several temperatures (solid circles) is fitted with a Curie law (thick line).

3.3. High-field linear susceptibility

Table 1 illustrates the temperature and field region where particles or clusters with different sizes of magnetic moments start to saturate. For any kind of moment, the magnetization is linear with applied field, if $\mu H/k_B T \ll 1$. The small Fe clusters ($15.9\mu_B$) fit the high-temperature limit for $T > 50$ K for fields of 10 kOe or less. At 4.6 K, the high-temperature approximation is no longer valid for these few-Fe-ion clusters. We have separated the Curie term from the paramagnetic background as given in (3.2). The high-field susceptibility at 4.6 K in figure 8 is the value without the contribution of these small clusters, which have saturated at this temperature.

Except for the data point at 4.6 K the high-field susceptibility has been represented by the thick black line in figure 8. Clusters of a few ions can explain the behaviour qualitatively, although the Curie constant calculated from the Brillouin function fit in figure 7 is just two-thirds of the fitted value from figure 8. The enhancement of the high-field susceptibility by a factor of 1.5 at 4.6 K (466 μemu mol^{-1}) over the room-temperature value (298 μemu mol^{-1}) may be due to the enhancement of Pauli paramagnetism.

3.4. The temperature dependence of the total magnetization

The Curie–Weiss fit of the total magnetic susceptibility with negative Θ is given in figure 8 (thin line). The parameters are given in table 2. The physical meaning of this negative Θ is rather curious. We discuss several models that might explain this.

Although it has been reported that the Pauli paramagnetism of some Fe–Zr alloys near 33 at.% Fe was enhanced by an order of magnitude due to the Stoner enhancement [13, 14], Stoner enhancement cannot account for the Curie–Weiss behaviour of the total susceptibility shown here. The Stoner enhancement of paramagnetism itself is, generally, only weakly temperature dependent, because the temperature dependence only originates from the thermal smearing of the Fermi function. The contribution from the Brillouin function term in (3.2), which is linear with H at high temperatures, to the high-field susceptibility is much larger than the change in the Pauli part. (See the difference of total susceptibility and $\chi_0 (= \chi_{\text{Pauli}} + \chi_{\text{dia}} + \chi_{\text{Van Vleck}})$ at 4.6 K in figure 8). Furthermore, even if the ferromagnetic transition occurs, the Stoner picture gives a $(T^2 - \Theta^2)^{-1}$ dependence, rather than the Curie–Weiss-like behaviour, $(T - \Theta)^{-1}$.

The quantum correction to the density of states by the electron–electron interaction via diffusion channels cannot explain the decrease of magnetic susceptibility with temperature. Although Kokanović *et al* [15] argued that a $-\sqrt{T}$ dependence of the susceptibility due to the electron–electron interaction is responsible for the initial negative slope of χ for $(Zr_{0.60}Cu_{0.40})_{1-x}H_x$ alloys below 100 K, spin fluctuations in the Fe–Zr alloy near the ferromagnetic transition limit [16] will reduce this contribution. Moreover, this quantum correction is much less than the observed change for the $Fe_{0.33}Zr_{0.67}$ alloy. Bakonyi [17] suggested that the Curie behaviour of superparamagnetic particles embedded in the amorphous non-magnetic matrix is responsible for the decrease of magnetic susceptibility with temperature, but this is not sufficient to explain the temperature dependence of the total magnetic susceptibility of $Fe_{0.33}Zr_{0.67}$, because $\sigma(T)$ in figure 4 is much less than the total magnetization at all temperatures.

Work by Dobrosavljević *et al* [18] suggests a way that might avoid the negative Θ of the Curie–Weiss law. They calculated the probability distribution $P(T_K)$ for Kondo temperatures related to the local fluctuations induced by localization effects in a dirty metal and concluded that the local $P(T_K)$ is sufficiently singular to induce a diverging magnetic susceptibility χ as T goes to zero, which is a non-Fermi-liquid behaviour. In their calculation, the $(1/T)$-dependent paramagnetic susceptibility has a correction, due to the increase of the effective

number of free spins, $\chi \sim n_{fr}(T_K)/T$, with $n_{fr}(T) \sim T^{\alpha(T)}$, where $\alpha(T) \to 0$ as $T \to 0$, but more slowly than any power law. They also predicted that $n_{fr}(T_K)$ becomes 40–60% for the temperature range 10^{-4}–1 K for highly disordered metals. The temperatures at which we studied $\chi(T)$ were larger than 10 K. Therefore the power of T for $n_{fr}(T)$ is not necessarily close to zero, but can be fixed to a constant power over the temperature region in which we are interested. The total magnetization at 10 kOe was also fitted to the power law including the Pauli, diamagnetic and Van Vleck susceptibilities, χ_0, as background

$$\chi = C/T^p + \chi_0. \tag{3.4}$$

A better fit was obtained than for the Curie–Weiss law ($\chi = C/(T - \Theta) + \chi_0$), with $p = 0.576$ and $\chi_0 = 183$ μemu mol^{-1} ($\chi_{Pauli} = 128$ μemu mol^{-1}). Furthermore, this value of the bare Pauli susceptibility is very close to those reported for $Cu_{0.33}Zr_{0.67}$ (118.9 μemu mol^{-1}), $Ni_{0.33}Zr_{0.67}$ (140.7 μemu mol^{-1}) and $Co_{0.33}Zr_{0.67}$ (149.9 μemu mol^{-1}) [13], which are of approximately the same magnitude, because the states near the Fermi level are dominated by Zr in each of these alloys [6]. Dobrosavljević *et al*'s calculation for the Kondo impurity is thus a good candidate to explain the temperature dependence of χ for $Fe_{0.33}Zr_{0.67}$ also.

4. Conclusion

We have studied the superparamagnetic nanoparticles embedded in the $Fe_{0.33}Zr_{0.67}$ alloy by conducting low-field magnetization measurements at several temperatures. Though the total saturation increases as T decreases, a maximum peak of the effective single-particle moment was found at 50 K, near the temperature at which the zero-field-cooled and field-cooled data split, 45 K. We expect that this temperature is the blocking temperature for the moments of the embedded particles. Observations of a reasonable coercive force below the blocking temperature also support the existence of these superparamagnetic nanoparticles with average moments of thousands of μ_B. However, the net saturation of these clusters is negligible compared to that of the local moments of few-Fe clusters (or Stoner-enhanced single Fe ions). We suggest that clusters of only a few Fe moments produced through direct Fe–Fe contact are responsible for the non-linear M–H curve at 4.6 K. The magnetic moment of these few-Fe clusters also qualitatively explains the temperature dependence of the high-field magnetic susceptibility. Values of the total susceptibility measured at 10 kOe are fitted to both the Curie–Weiss law and a power of T plus a constant; the power law gives a better statistical fit than the Curie–Weiss law. Thus larger superparamagnetic particles embedded in the $Fe_{0.33}Zr_{0.67}$ alloy system generate the non-linear M–H plot at low field and temperatures from 10 K to 100 K, but the small Fe clusters dominate the strong temperature dependence of the total magnetic susceptibility, and high-field non-linearity of M against H at 4.6 K.

Acknowledgments

The work at the Univeristy of Manitoba was partially financed by the Natural Sciences and Engineering Research Council of Canada, that at the University of Texas by the National Science Foundation (DMR9158089) and the Robert A Welch Foundation (F-1191), and that at Texas A&M University by the Robert A Welch Foundation (A-0514).

References

[1] Michaelsen C, Wagner H A and Freyhardt H C 1986 *J. Phys. F: Met. Phys.* **16** 109
[2] Ryan D H, Coey J M D, Batalla E, Altounian Z and Ström-Olsen J O 1987 *Phys. Rev.* B **35** 8630
[3] Saito N, Fukamichi K and Nakayawa Y 1990 *Sci. Rep. (Research Institutes Tohoku University Series, Chemistry and Metallurgy (Japan))* **35** 65
[4] Gupta S N and Verma H C 1988 *Phys. Status Solidi* a **105** 275
[5] Krebs H U, Biegel W, Bienenstock A, Webb D J and Geballe T H 1988 *Mater. Sci. Eng.* **97** 163
[6] Trudeau M, Cochrane R W, Baxter D V, Ström-Olsen J O and Muir W B 1988 *Phys. Rev.* B **37** 4499
[7] Hedman L and Rapp Ö 1984 *Phys. Lett.* **100A** 251
[8] Bakonyi I, Varga L K, Lovas A, Tóth-Kádár E and Sólyom A 1985 *J. Magn. Magn. Mater.* **50** 111
[9] Bakonyi I, Panissod P, Miljak M and Babić E 1986 *J. Magn. Magn. Mater.* **58** 97
[10] Kanemaki S, Takehira O, Fukumichi K and Mizutani U 1989 *J. Phys.: Condens. Matter* **1** 5903
[11] Morrish A H 1965 *The Physical Principles of Magnetism* (New York: Wiley)
Morrish A H and Zhou X Z 1991 *Science and Technology of Nanostructured Magnetic Materials* ed G Hadjipanayis and G A Prinz (New York: Plenum) p 511
[12] Néel L 1947 *C. R. Acad. Sci.* **224** 1448
[13] Altounian Z and Ström-Olsen J O 1983 *Phys. Rev.* B **27** 4149
[14] Batalla E, Altounian Z and Ström-Olsen J O 1985 *Phys. Rev.* B **31** 577
[15] Kokanović I, Leontić B and Lukatela J 1990 *Phys. Rev.* B **41** 958
[16] Ström-Olsen J O, Altounian Z, Cochrane R W and Kaiser A B 1985 *Phys. Rev.* B **31** 6116
[17] Bakonyi I 1992 *Phys. Rev.* B **45** 5066
[18] Dobrosavljević V, Kirkpatrick T R and Kotliar G 1992 *Phys. Rev. Lett.* B **69** 1113